Investigation of the local environment of hydrophobic end-groups on polyethylene glycol (PEG) brushes using fluorometry: relationship to click chemistry conjugation reactions on PEG protected nanoparticles

Christopher V. H.-H. Chen, Brian P. Triana, and Robert K. Prud'homme*

Department of Chemical and Biological Engineering, Princeton University, Princeton, New Jersey 08540, United States
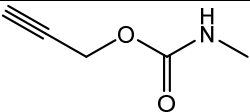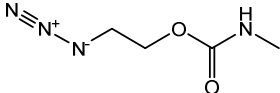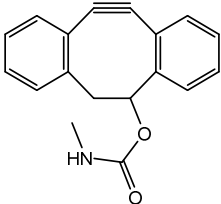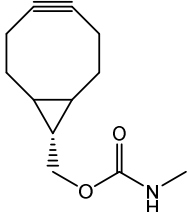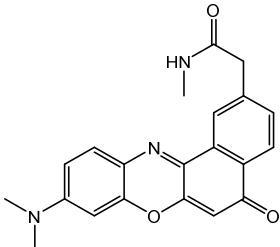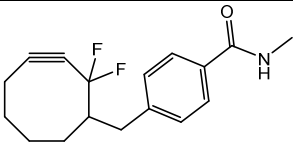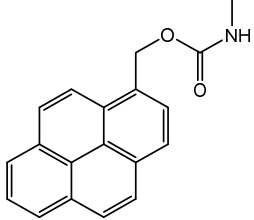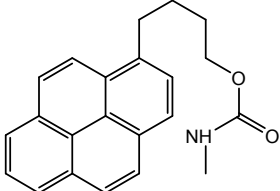*Author for correspondence. E-mail: prudhomm@princeton.edu

SI-I. Calculation of Octanol-Water Partition Coefficients (LogPs)

The calculation of octanol-water partition coefficients (LogPs) are done for the N-methylamide derivative of carboxylic acids and the N-methyl carbamate derivatives of alcohols, similarly to how Debets, et al. had calculated the logPs of their hydrophobic strain promoted cyclooctynes[1]. Molinspiration's Molecular Properties and Bioactivity Score calculator was used to determine logP values. Table S1 contains the structures of which we calculated the LogPs, shown in Table 1. Here we use LogP as a measurement of the hydrophobicity of the functional end-group and a means to order the effects of hydrophobicity on end-group location.

SI-II. Synthetic Procedures

General. All reagents used were obtained from commercial sources and used without further purification, unless specified. 1,6-dihydroxynaphthol (99%) was purchased from Acros Organics, and 5-dimethylamino-2-nitrosophenol hydrochloride (>98%) was purchased from TCI as precursors to our hydroxy-Nile Red derivative (9-dimethylamino-2-hydroxy-5H-benzo[a]phenoxazin-5-one). Poly(styrene-b-ethylene oxide) (PS-PEG) block copolymer of a variety of sizes and 1.8k polystyrene (PS) were ordered from Polymer Source. Triethylamine (TEA, 99.5%), methanesulfonyl chloride (>99.7%), pyrene (99%), 1-pyrenemethanol (99%), and 1-pyrenebutanol (98%) were all obtained from Sigma-Aldrich. All solvents

Table S1. Comparison of Octanol-Water Partition Coefficients (LogPs) of Functional End-Groups as Calculated via Molinspiration with Structures

| End-Group	LogP	Structure
Alkyne	0.3	
Azide	0.9	
DBCO (Dibenzocyclooctynes)	2.9	
BCN (Bicyclo-[6.1.0]-nonyne)	3.0	
Nile Red (NR)	3.2	
DIFO2 (Difluorinated Cyclooctyne 2)	4.3	
Methylpyrene (PyM)	4.4	
Butylpyrene (PyB)	5.7	

used were of ACS grade (or higher) and were purchased from Fisher. Column chromatography was performed using Fluka basic alumina, Brockmann activity I (60-350 mesh). Molecules were characterized by ^{1}H NMR on a 500 MHz Bruker Ultra Shield Plus in DMSO-d6.

Scheme 1. Synthesis of mesyl-terminated poly(styrene-b-ethylene oxide) (**B**).
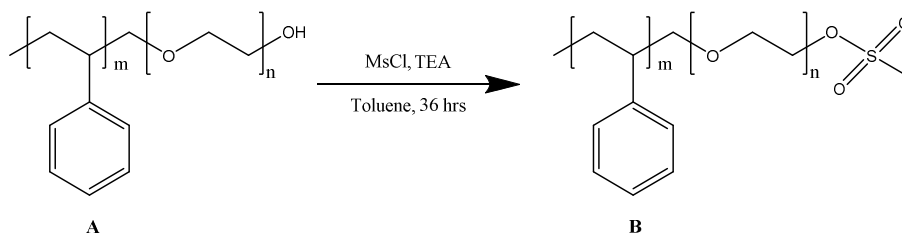
Mesyl-terminated Poly(styrene-b-ethylene oxide) (PS-PEG-OMs) (B). Dye functionalized PS-PEG was synthesized by first synthesizing the methanesulfonyl (mesyl) derivative of PS-PEG (**A**). 100 mg of copolymer was added to 40 mL toluene in a 50 mL round bottom flask. In order to dry the polymer, water was removed via azeotropic distillation of the PS-PEG in toluene solution at around 130 $^{\circ}$C. After 30 mL of solvent was removed, 20 mL anhydrous toluene was added to the flask and distillation is allowed to continue. Once another 20 mL of liquid is distilled, the reaction flask was brought back down to room temperature and sealed. 10 eq. of distilled TEA was then added, and the reaction flask was purged with argon for 15 minutes. 20 eq. of methanesulfonyl chloride (MsCl) were added after purging dropwise, and the reaction was carried out for 36 hours, stirring at room temperature. The reaction solution was then filtered with a 0.22 µm nylon filter to remove TEA salts, and then concentrated to 2 mL by rotary evaporation prior to precipitation dropwise into 100 mL cold diethyl ether. The precipitate was filtered and dried in vacuo overnight. See Figure S1 for an example ^{1}H NMR. PS-PEG lengths used were 3.5k-b-5.5k, 3.6k-b-16.6k, 3.6k-b-25k, 3.7k-b-36k, and 3.6k-b-67k. 5k monomethyl PEG was also transformed to monomethyl mesyl PEG (PEG-OMs) in this way, to similar yield. Typical yield of ~80%.

Scheme 2. Synthesis of 9-Dimethylamino-2-hydroxy-5H-benzo[a]phenoxazin-5-one (**E**).
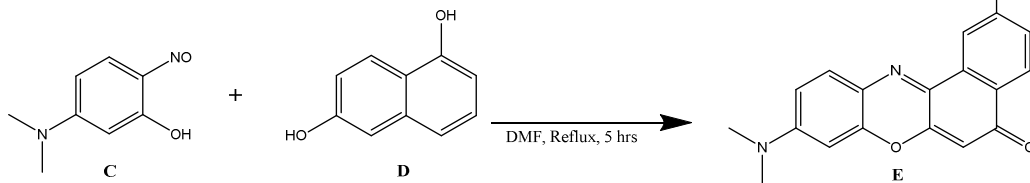

*9-Dimethylamino-2-hydroxy-5H-benzo[a]phenoxazin-5-one (HOMe$_2$NR, **E**).* 1,6-dihydroxynaphthol (**D**) (208 mg, 1.026 mmol) and 5-dimethylamino-2-nitrosophenol hydrochloride (**C**) (246 mg, 1.54 mmol) were reacted under reflux in 20 mL DMF in a 50 mL round bottom flask for 5 hours. The DMF was then removed with the aid of added heptane (heterogeneous azeotropic distillation[2]) to near dryness. The reaction solution was not dried completely because the synthesized analogue of Nile Red is difficult to resolubilize and recover when dried. This concentrated crude mixture was purified via flash chromatography with 2:1 ethyl acetate-isopropanol to yield a vibrant red solution that dries to a black, green solid (95.1 mg, 28% mass recovery). Much of the product can be visibly seen still on the column, but flash chromatography is typically stopped after 8 hours. Fluorescence spectra of dried product in toluene and methanol found to be similar to that of pure Nile Red when excited at 514 nm. Procedure adapted from Briggs, et al[3]. See Figure S2 for ^{1}H NMR.

*Nile Red-functionalized Poly(styrene-b-ethylene oxide) (PS-PEG-NR) (**F**).* 50 mg PS-PEG-OMs was added to 20 mL toluene in a 50 mL round bottom flask, and dried via azeotropic distillation at around 130 °C. After 10 mL of solvent was removed, 10 eq. of TEA and 10 eq. of HOMe$_2$NR were added the flask. The reaction was carried out stirring for 48 hours under toluene reflux. The solution was then concentrated to 2 mL by rotary evaporation before added dropwise to 100 mL cold ether to precipitate product. Precipitate was filtered and dried in vacuo overnight. See Figure S3 for ^{1}H NMR. Some residual salts and other impurities are seen in ^{1}H NMR between 4-5 ppm, which could be removed by washing with water, but are not as extraction of product from water is difficult due to the surface activity of PS-PEG. Typical reaction yield of

around 60% PS-PEG-NR was seen for the Nile Red-tethered PS-PEG. 5k PEG-NR, a water soluble analogue

of Nile Red, was also synthesized in this fashion from 5k PEG-OMs with similar yield.

Scheme 3. Synthesis of dye functionalized poly(styrene-b-ethylene oxide) Nile Red-functionalized PS-PEG (**F**), methylpyrene-functionalized PS-PEG (**H**), and butylpyrene-functionalized PS-PEG (**J**).
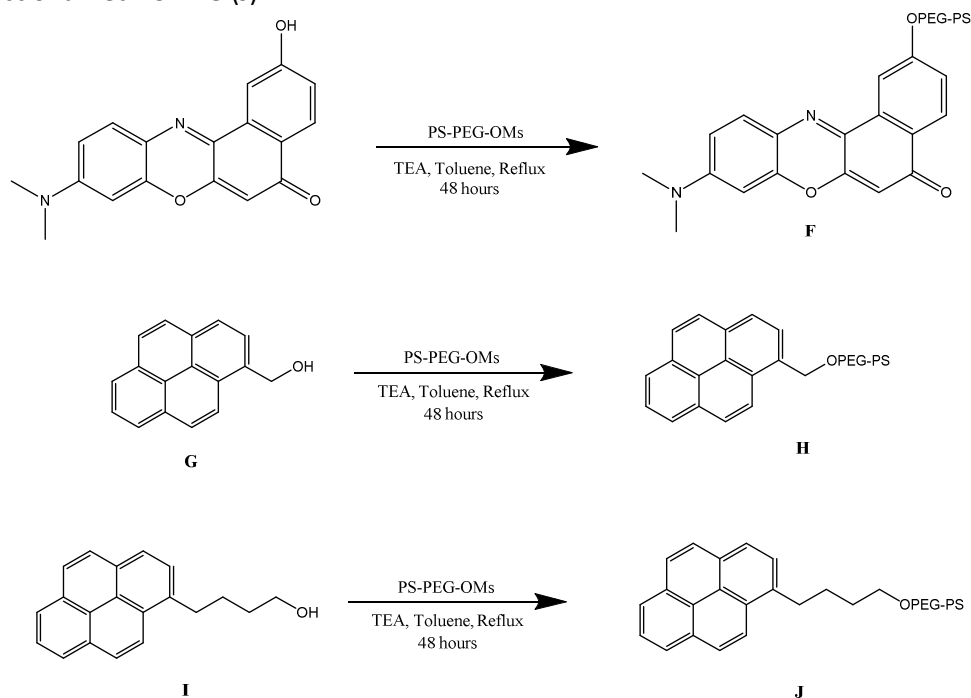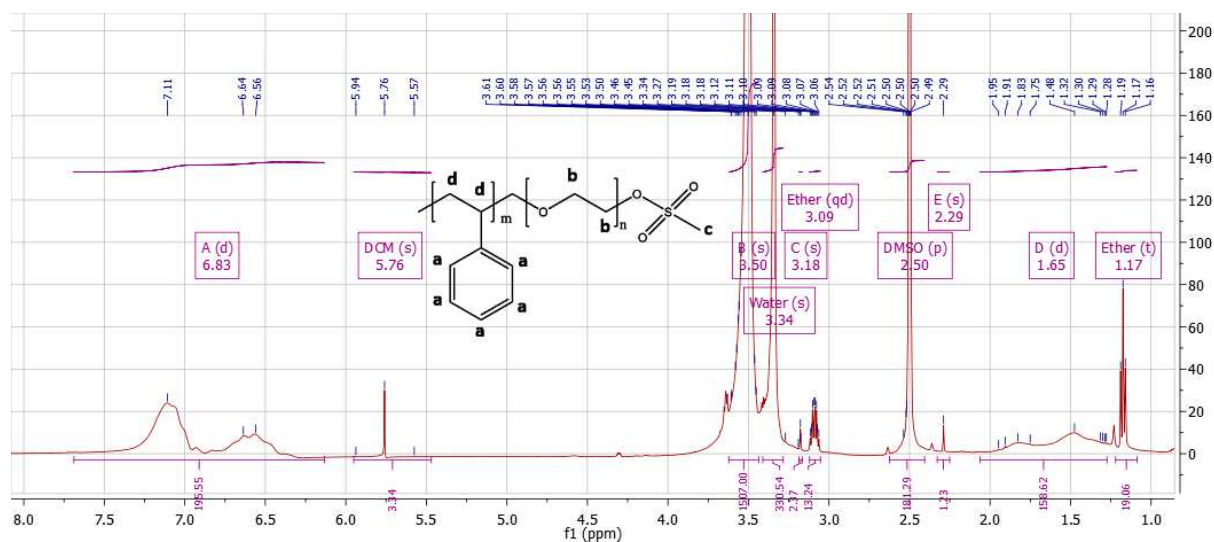

Pyrene-functionalized Poly(styrene-b-ethylene oxide). Two different Pyrene (Py)-functionalized PS-PEGs

were synthesized for this study: methylpyrene (PyM)-functionalized PS-PEG (PS-PEG-OPyM, **H**) and

butylpyrene (PyB)-functionalized PS-PEG (PS-PEG-OPyB, **J**). The only difference in syntheses was the

addition of either 1-pyrenemethanol (**G**) or 1-pyrenebutanol (**I**). For both, 50 mg of PS-PEG-OMs was

added to 20 mL toluene in a round bottom flask and dried by azeotropic distillation. After 10 mL of solvent

was removed, 10 eq. of TEA and 10 eq. of pyrene derivative were added. The reaction stirred under reflux

for 48 hours. The solution was concentrated to 2 mL by rotary evaporation before precipitation dropwise

into 100 mL cold ether. Precipitate filtered and dissolved into 100 mL DCM. This DCM solution was

concentrated to 2 mL by rotary evaporation before second precipitation into 100 mL cold ether.

Precipitate is filtered and dried under high vacuum overnight. A typical yield of around 50% was observed

for the pyrene-functionaliztion of PS-PEG. See Figure S4 for a sample ^{1}H NMR of PS-PEG-OPyB. Some residual salts and other impurities are seen in ^{1}H NMR between 4-5 ppm, which could be removed by washing with water. These pyrene derivative-termined PS-PEGs were used for the pyrene-tethered NP experiments.

Nanoparticle Formation. Nanoparticles (NPs) were generated via Flash NanoPrecipitation (FNP) as described by Han, et al. using a two-inlet vortex mixer[4]. The THF stream contained 1.8k PS (7.5 mg/mL) and PS-PEG (12.5 mg/mL) was quickly mixed by impinging this stream with a pure water stream at a 1:1 volume ratio. Py derivative-tethered experiments contained 3.4 µg/mL pyrene in the THF stream. NR-tethered NPs contained 4 mg/mL PS-PEG-NR (12-93 µg/mL NR) and 8.5 mg/mL PS-PEG, of the same PEG block M_{w}, to reach the same PS-PEG mass concentration used in the other NP experiments. The resultant mixture was collected in a water bath to dilute the final THF concentration to 10 v%. THF was removed by dialysis in water in a 1:400 volume ratio in a Spectra/Por regenerated cellulose bag with 6-8k molecular weight cut off, changing the dialysis water every hour for the first 6 hours before letting the solution dialyze overnight. The NP solutions were concentrated over silica gel. NPs were sized by DLS, on a Malvern Zetasizer Nano-ZS, and solution concentration was determined by TGA using a TA Instruments Q50 thermogravimetric analyzer courtesy of the Priestley group at Princeton University.

SI-III. NMR Spectra

Figure S1. Example ^{1}H NMR of mesyl-terminated poly(styrene-b-ethylene oxide) (3.6k-b-16.6k) (**B**).
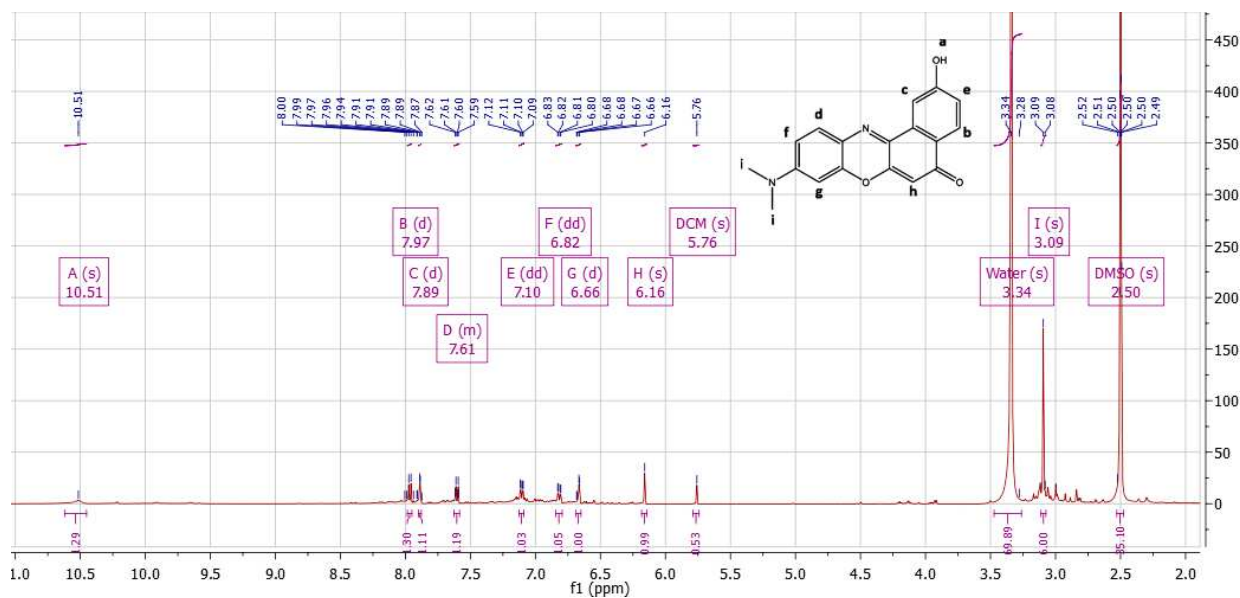
Figure S2. ^{1}H NMR of 9-Dimethylamino-2-hydroxy-5H-benzo[a]phenoxazin-5-one (**E**).
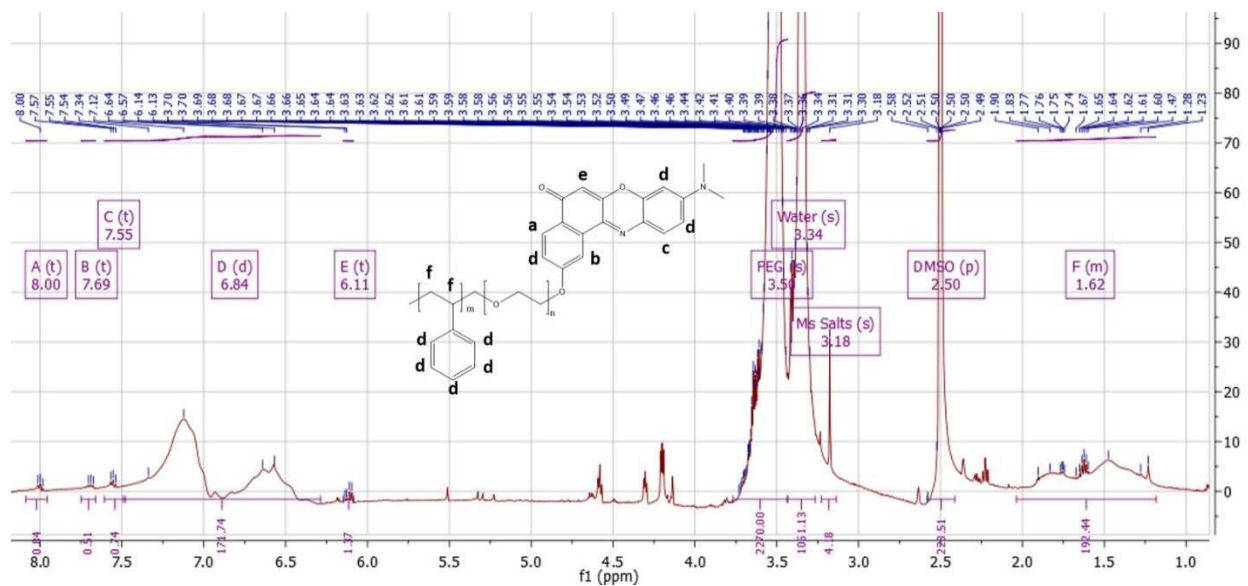
Figure S3. Example ^{1}H NMR of Nile Red-functionalized poly(styrene-b-ethylene oxide) (3.6k-b-25k) (**F**). Impurities are seen at 4.2 and 4.7 ppm, which are discussed in length in SI-VIII.
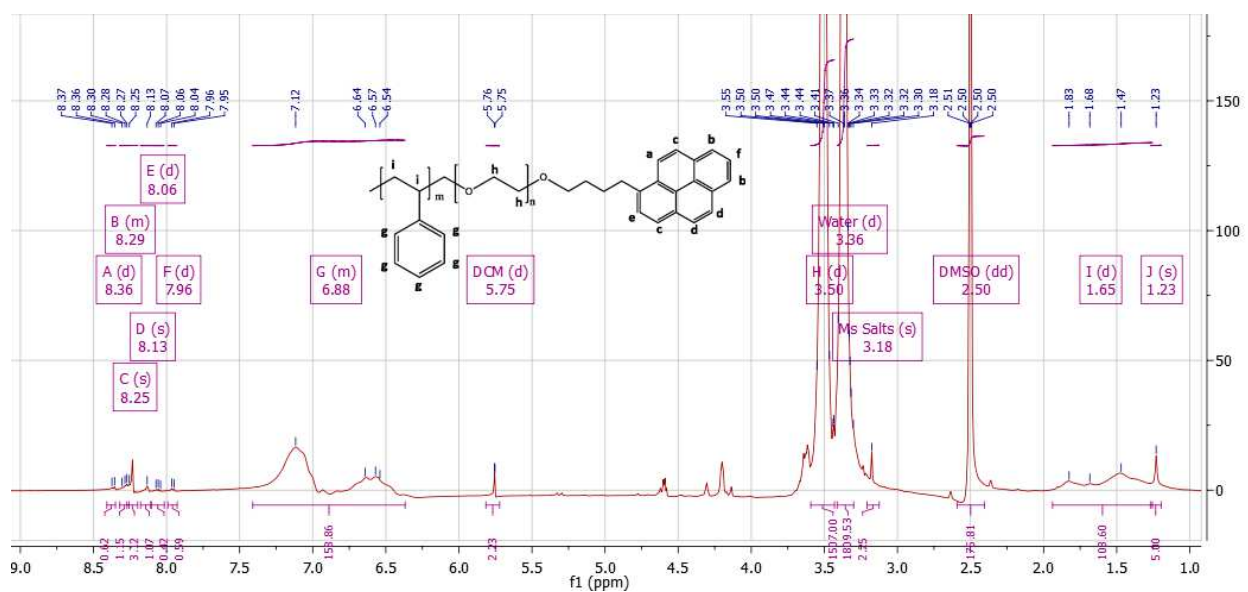
Figure S4. Example ^{1}H NMR of butylpyrene-functionalized poly(styrene-b-ethylene oxide) (3.6k-b-16.6k) (**H**). Impurities are seen at 4.2 and 4.7 ppm, which are discussed in length in SI-VIII.

SI-IV. Nanoparticle Characterization

DLS measurements were taken using a Malvern Zetasizer Nano ZS at room temperature in aqueous solutions that were water clear. Reported Z-average diameters and polydispersity indices (PDIs) are averages over 3 runs of the same sample from the intensity weighted size distribution.

Table S2. Nile Red Nanoparticle DLS Sizing Data

Copolymer (PS-PEG)	Nanoparticle Type	Z-average Diameter (nm)	Polydispersity Index
3.5k-b-5.5k	Unloaded	66.4	0.397
	Tethered	81.1	0.442
3.6k-b-16.6k	Unloaded	92.5	0.277
	Tethered	116	0.261
3.6k-b-25k	Unloaded	146	0.244
	Tethered	164	0.258
3.7k-b-36k	Unloaded	67	0.057
	Tethered	138	0.265
3.6k-b-67k	Unloaded	135	0.359
	Tethered	135	0.125

Table S3. Pyrene-Tethered Nanoparticle DLS Sizing Data

Copolymer (PS-PEG)	Nanoparticle Type	Z-average Diameter (nm)	Polydispersity Index
3.5k-b-16.6k	Unloaded	56.98	.068
	Methylpyrene	92.45	.364
	Butylpyrene	114.6	.236

SI-V. Fluorescence Data

Nile Red. Fluorometry was conducted using a Hitachi F-7000 FL Spectrometer. For all Nile Red experiments, samples were excited at 514 nm, using 10 nm slits, scan speed of 1200 nm/min, and a PMT voltage of 250 V. Figure S5 shows the emission of NR in various environments. 5k PEG-NR being used to take the emission spectrum of NR in water, because NR is otherwise insoluble in water. Where as in Figure 2, in which only

the spectra for toluene, ethanol, and water are given for environments similar to that of NR encapsulated in the core, captured in the corona, or presented at the surface of the PS-PEG NP, respectively, we show spectra over a series of environments from water to ethanol to toluene. These results mirror those found by Jose and Burgess[5]. There is a large intensity increase from NR in water to ethanol, where toluene and ethanol are more similar in intensity. The difference between the apexes of the emission spectra in water and toluene is nearly 100 nm, as can be seen in the inset of Figure S5. Though, of greater significance is the difference in the shifts in the emission spectra between water to ethanol, which is relatively gradual, to that of ethanol to toluene. This allows for us to confidently distinguish between the fluorescence of NR in core-like environments of our PS-PEG NPs as compared to that in the corona or at the surface.
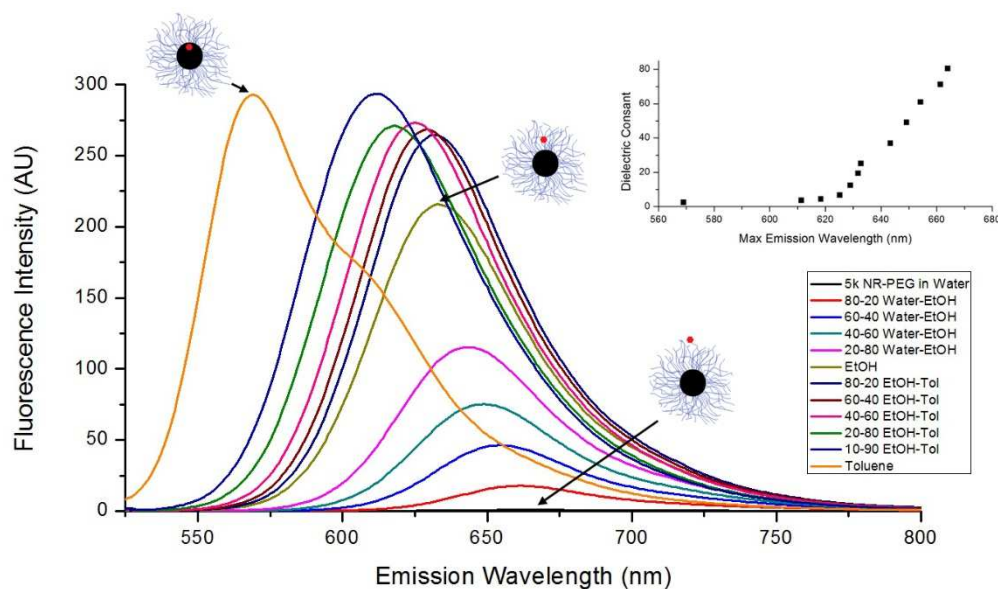
Figure S5. Non-normalized Nile Red emission spectra of 1 µg/mL dye in binary solutions of water-ethanol and ethanol-toluene in volume ratios. A more gradual change in spectra is noticed between water and ethanol compared to ethanol and toluene. **(Inset)** The emission peaks versus the dielectric constant of the environment. There is more than a 50 nm shift in emission peak between 10 v% ethanol in toluene relative to that of pure toluene, which allows for a reliable means of discerning NR in PS-PEG NP core-like environments from NR in the corona.
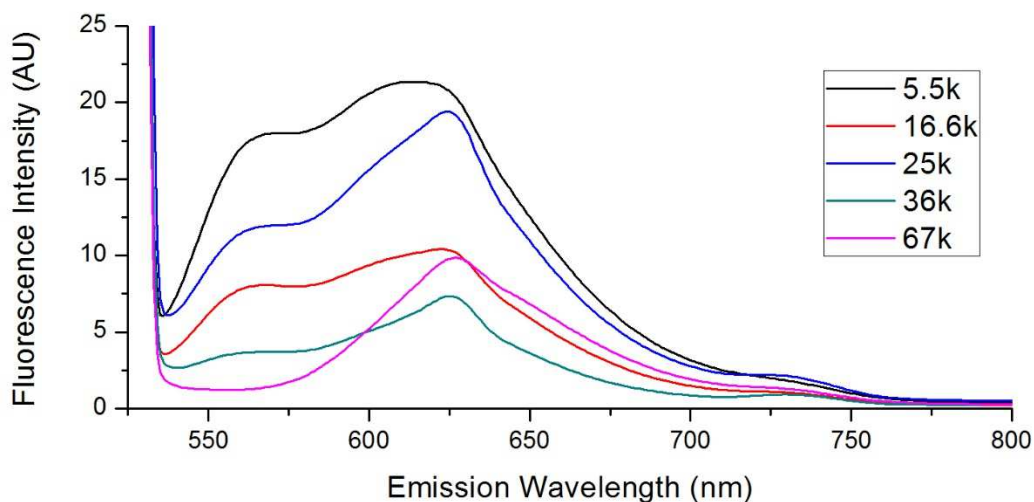
Figure S6. Non-normalized emission spectra of 0.1 w% (1 mg/mL) Nile Red-tethered NPs in water. Molecular weights of the PEG chain lengths of the PS-PEGs used are shown in the legend. PS block M_Ws were 3.6k $\pm$ 0.1k. Differences in fluorescence intensity are due to differences in NR loading between samples due to a constant 4.0 mg/mL PS-PEG-NR in THF during NP synthesis invariant of PEG blow M_W.

Figure S6 is the non-normalized version of Figure 3. There is a clear trend in reduction of the fluorescent population in the core when moving to larger PEG chain lengths. Corona-like emission peaks are seen between 615-627 nm, increasing with PEG chain length, similar to NR emission in 20 to 40 v% ethanol in toluene. This suggests that NR is sampling a more hydrophobic environment than the PEG corona, or that the PEG corona is more hydrophobic than ethanol, a topic discussed further in SI-VII.

Pyrene. For all Py experiments, samples were excited at 335 nm, using a 5 nm excitation slit and 1 nm emission slit, scan speed of 240 nm/min, and a PMT voltage of 700 V. Figure S7 shows the normalized and raw data for the PyM- and PyB-tethered NPs 1 mg/mL in water (0.1 w%) and 0.01 mg/mL 1-pyrenemethanol and 1-pyrenebutanol in toluene. These figures demonstrate how closely the emission spectra of the free dye in toluene and the dyes tethered to PS-PEG NPs are similar in their fluorescence spectra, suggesting that the dye is mostly sampling a toluene or core-like environment. Figure S8 shows the normalized data for 1-pyrenemethanol and 1-pyrene butanol in binary solutions of ethanol in toluene. Here we see that the I1/I3 ratio or polarity parameter generally increases when the dye is solvated in a

more hydrophobic environment (greater volume of toluene in solution). However, as seen in Figure 5, the polarity parameter is relatively constant for both dyes for binary solutions of 5-25 v% ethanol in toluene. For this reason, the calculation to determine the percentage of the dye that resides in the core of the NP is done by linearly extrapolating between pure toluene and 5 v% ethanol in toluene, instead of between pure toluene and pure ethanol.

Non-linear curves of polarity parameter versus solvent concentration (see Figure 5) have been seen previously for other binary solvent mixtures, such as tetrahydrofuran or acetonitrile in water[6]. Thus, our results for the polarity parameters Py derivatives in ethanol-toluene mixtures are reasonable.
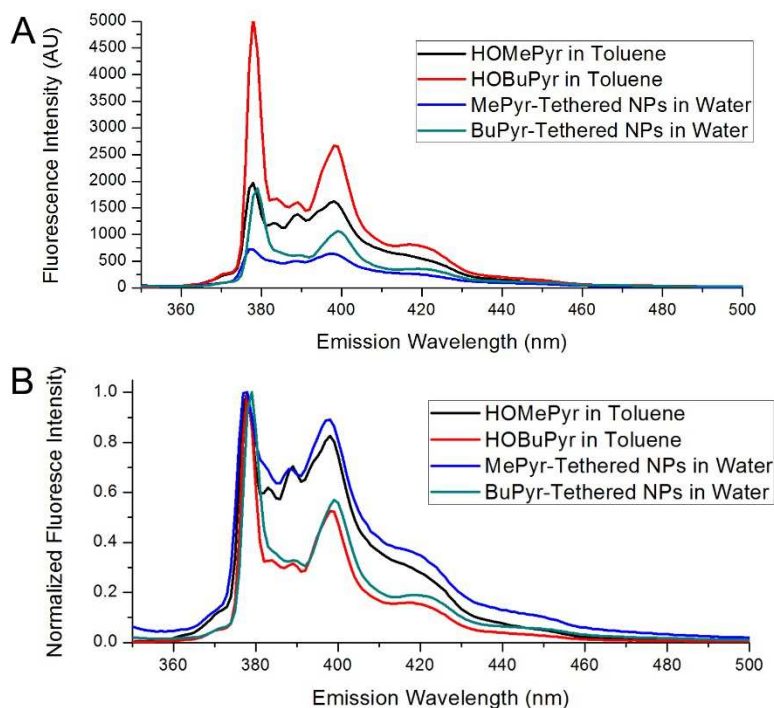
Figure S7. (A) Non-normalized and **(B)** Normalized fluorescence emission data of 0.01 mg/mL pyrene-derivative free in toluene or 1 mg/mL derivative-tethered NPs in water.
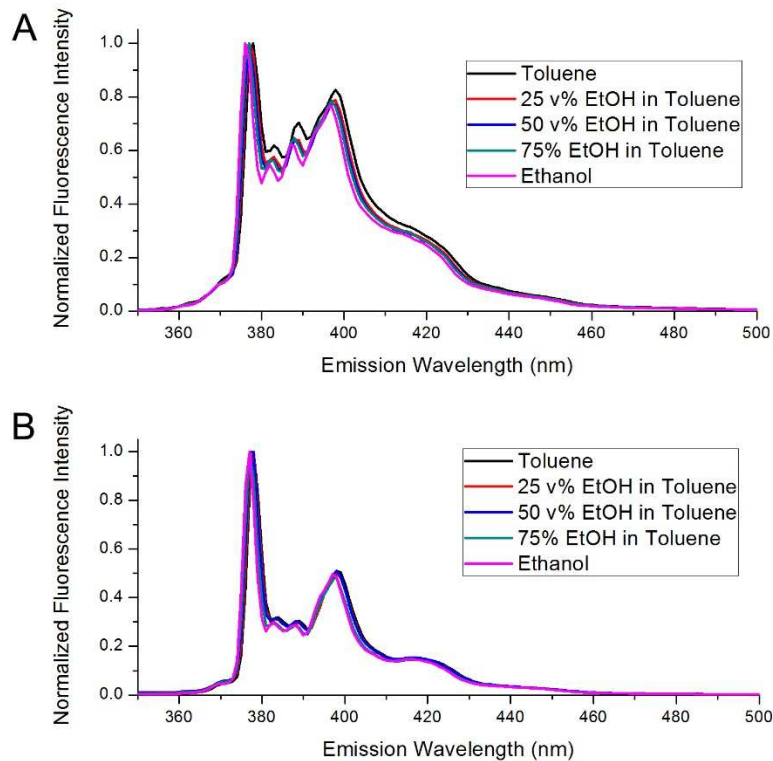
Figure S8. (A) 1-pyrenemethanol and **(B)** 1-pyrenebutanol in binary solutions of ethanol and toluene. As the solutions become more hydrophobic (greater toluene fractions) the I1/I3 ratios become smaller.

SI-VI. Deconvolution of NR Fluorescence Emission Spectra

We find the distribution of dye across the three NP environments – PS core, PEG corona, and corona-aqueous interface – by using the following linear superposition model:

$$I_{conv} = a_{Core}I_{Tol} + a_{Corona}I_{EtOH} + a_{Aqueous}I_{Water}$$

where I_{conv} is the convolved fluorescence spectra, I_{Tol}, I_{EtOH}, I_{Water}, are spectra representing the NP core, corona, and corona-aqueous interface, as in Figure 3, and a_{Core}, a_{Corona} and $a_{Aqueous}$ are constants that we use to vary the weights of the corona and corona-aqueous interface spectra. As seen in Figure S5, the maximum emission intensities of NR in each of these environments are different, and this model takes this into account by using non-normalized, emission spectra to generate the convolution spectra. To optimize the constants a, the resultant I_{conv} is normalized against its own maximum intensity and then compared against the normalized measured fluorescence spectra of NR-tethered NPs in water. The

weighting constants are then varied either to maximize R^2 (resulting in the data shown in Figure 4) or to minimize the difference between the intensities of the convolution and measured data where the core-like peak is expected (at 569 nm). Excel's Solver function is then used to vary a_{Corona} and $a_{Aqueous}$, relative to a_{Core}, which is set to 1. The relative concentration (in percent) of the dye in each environment can be found by finding the contribution of $a_{Environment}$ relative to the sum of all a. Table S4 and S5 show the optimized values of a maximizing R^2 or minimizing the core peak difference, respectively. The latter fit favors NR in the corona by 5-7%. Figure S9 compares the normalized measured spectra of NR-tethered 3.6k-b-25k NPs in water to the model using the two fits.

Table S4. Optimized Fit Parameters when Maximizing R^2

| PEG M$_W$ | a_{Corona} | $a_{Aqueous}$ | NR Concentration (%) in | | | R^2 |
			Core	Corona	Interface	
5.5k	0.744	0	57.3	42.7	0	0.958
16k	0.991	0	50.2	49.8	0	0.942
25k	1.1	0	47.7	52.3	0	0.906
36k	1.42	0	41.4	58.6	0	0.874
67k	6.2	0	13.9	86.1	0	0.964

Table S5. Optimized Fit Parameters when Minimizing the Core Peak Difference

| PEG M$_W$ | a_{Corona} | $a_{Aqueous}$ | NR Concentration (%) in | | | R^2 |
			Core	Corona	Interface	
5.5k	0.994	0	50.2	49.8	0	0.928
16k	1.32	0	43.1	56.9	0	0.915
25k	1.45	0	40.8	59.2	0	0.877
36k	1.88	0	34.8	65.2	0	0.846
67k	10.4	0	8.7	91.2	0	0.953
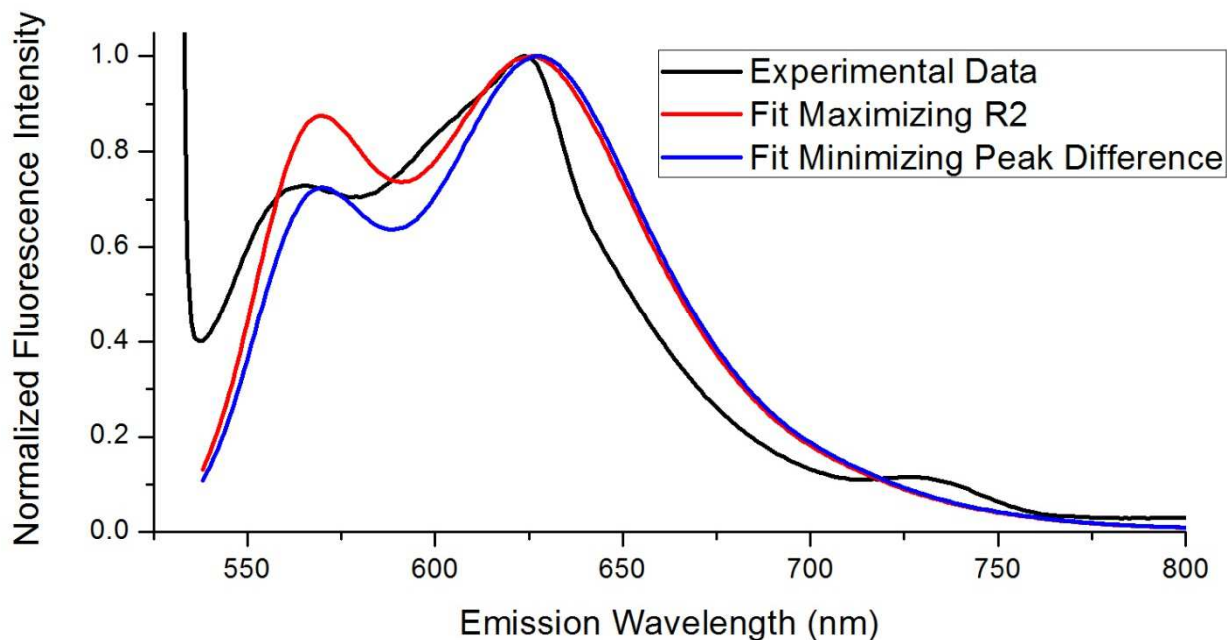
Figure S9. Comparison of the experimental data for 3.6k-b-25k NR-tethered PS-PEG NPs in water with the against the two fitting methods of maximizing R^2 or minimizing the core peak (569 nm) difference between the fit and the experimental data.

SI-VII. Discussion on the Approximation of NP Environments with Solvents

Nile Red. For both the NR and Py experiments, we use toluene to represent the PS core, ethanol to represent the PEG corona, and water to represent the NP corona-aqueous interface. Both toluene and ethanol were chosen to represent the core and corona, respectively, due to their similarities to PS and PEG. However, the differences in connectivity of the molecules may lead to differences between the fluorescence of the dye in the solvent analogue phase and the in the polymer phase. To assure that these phases are appropriate, we compared the fluorescence of NR in solutions of 20k PEG in ethanol (saturated) and 1.8k PS in toluene (20 mg/mL) to NR in pure ethanol and pure toluene. These experiments were taken at NR concentrations of 10 µg/mL using fluorometer settings as described in SI-V. We find that the fluorescence spectra of the solutions with and without polymer are very similar, with only slight differences in fluorescence intensity, as shown in Figure S10. Hence, we expect that ethanol and toluene are reasonable approximations of the NP PEG corona and PS core.
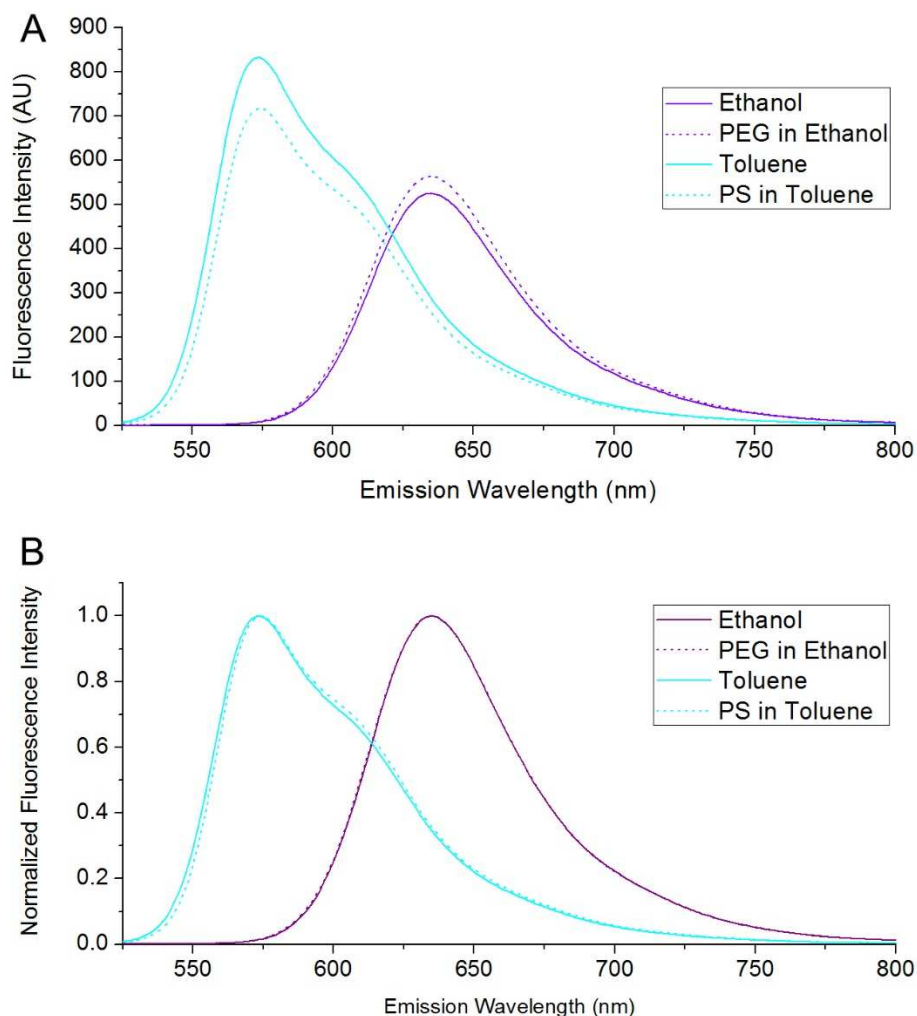
Figure S10. Comparison of the fluorescence spectra of NR in ethanol, saturated 20k PEG in ethanol, toluene, and 20 mg/mL PS in toluene (**A**) without normalization and (**B**) with normalization. Doping the solutions with polymer does not significantly change the fluorescence spectra.

When comparing the fluorescence of the NP with the ethanol or toluene, there is a slight deviation between the experimental and representatives peaks for the core and corona (as can be seen in Figure 3 and in the peak convolution discussion in Figure S9). For both environments, NR fluoresces in a more hydrophobic (lower wavelength) environment than the analogous solvent. The core-like peak is slightly blue shifted from the toluene peak (a 1-3 nm), which can be attributed to the contribution of the more hydrophobic alkyl backbone present in PS not captured by toluene. For PEG, some of the hydrophobic

shift is attributed to the shoulder of the NR emission spectrum in toluene at around 620 nm. This shoulder plays a greater role when the dye samples the core a greater percentage, as NR does in our tethered NPs at lower PEG block molecular weights. As expected, the corona-like peak in our NPs appears at a lower wavelength for lower PEG block M_Ws.

Since the PEG layer is not a solid-like PEG phase, but is instead a PEG layer permeated with water, we would expect NR in the corona to fluoresce like NR in PEG-water (or in our analogous case, ethanol-water) solutions than pure PEG. The content of PEG in water expected would be dependent on both the conformation of the PEG brush layer[7] and the location of the dye. To test this idea, we compared the fluorescence of 1 µg/mL NR in 6k PEG-, 20k PEG-, ethylene glycol-, and ethanol-water solutions, measured as described in SI-V, as shown in Figure S11. As expected, at low concentration of additives, NR fluoresces similarly to NR in water and decreases in emission peak wavelength as the solution becomes less water-like. The fluorescence of NR in the NP PEG corona is shown in Figure S11 to allow for the comparison of the observed NR fluorescence in the NP experiments with the potential approximating environments.

We do not find NR fluorescence to be similar to that of NR in 6k PEG-, 20k PEG-, ethylene glycol-, or ethanol-water solutions, and instead find corona fluorescence to be more similar to NR in pure ethanol or ethanol-toluene solutions. This suggests that NR is sampling a PEG environment that is excluding water, making the PEG phase more hydrophobic. Since NR is hydrophobic (logP = 3.2), this result is not unexpected. However, these NR-PEG aggregates would pose an additional resistance to interaction with the hydrophobic end group. The local PEG environment of the end group would need to be removed for direct contact with the functionality along with penetration of the PEG brush layer to allow for conjugation.
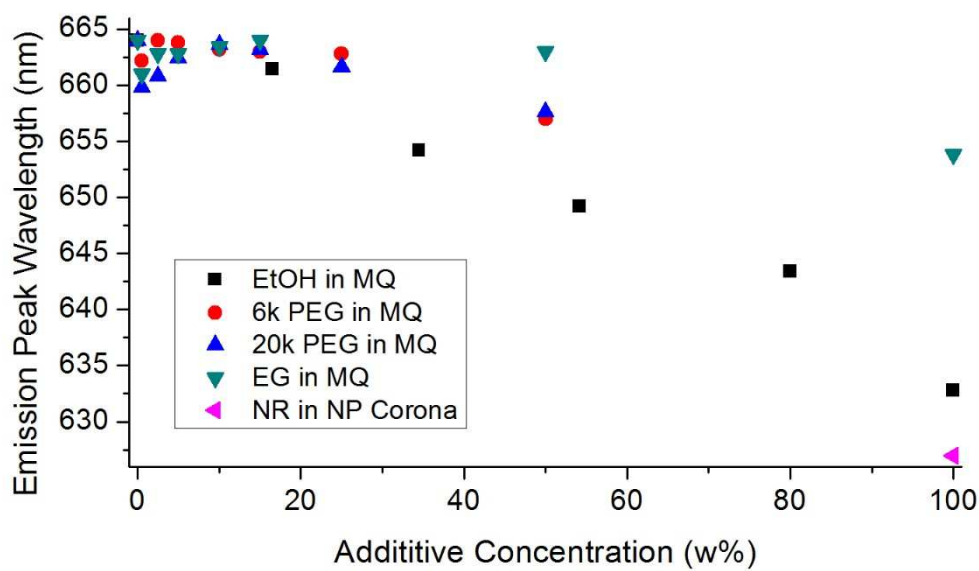
Figure S11. Comparison of the fluorescence emission peak wavelengths of 1 μg/mL NR in ethanol-, 6k PEG-, 20k PEG-, and ethylene glycol-water solutions against the measured fluorescence NR in NP (PEG) corona. NR in the NP corona fluorescence most similarly to NR in pure ethanol (or ethanol-toluene solutions).

Pyrene. Similar to NR, Py is observed to sample a more hydrophobic environment than toluene, as demonstrated in Figure 5 by the PyB-tethrered NP fluorescence in water. To determine whether an adjustment could be made by the addition of hexanes to toluene – in order to add the missing alkyl contribution present in polystyrene – the polarity parameters of binary mixtures of pyrenemethanol and pyrenebutanol in binary mixtures of toluene and hexanes were determined as described in SI-V. The results of these experiments are shown in Figure S12, showing a near linear trend for both dyes.

As expected, PyB-tethered NPs appear to have a similar polarity parameter to pyrenebutanol in toluene in hexanes. However, the concentration of toluene in hexanes (51 v%) was much lower than the expected 86% toluene in hexanes – the mass ratio of toluene to hexanes that would comprise polystyrene. Once again, the difference in hydrophobicities between the solvent analogues and the polymer can be attributed to the connectivity of the polymer, which allows for specific interactions between the dye and the polymer that are not captured by the approximating solvent solutions. If the core is in fact more

hydrophobic than the representative toluene phase, then the percentage of PyM in the core is overestimated. This could be balanced out by the underestimation of the PEG corona hydrophobicity, if, as we would expect, the Py derivatives sample a water-excluded PEG phase as NR does. PyB would still reside entirely in the core.
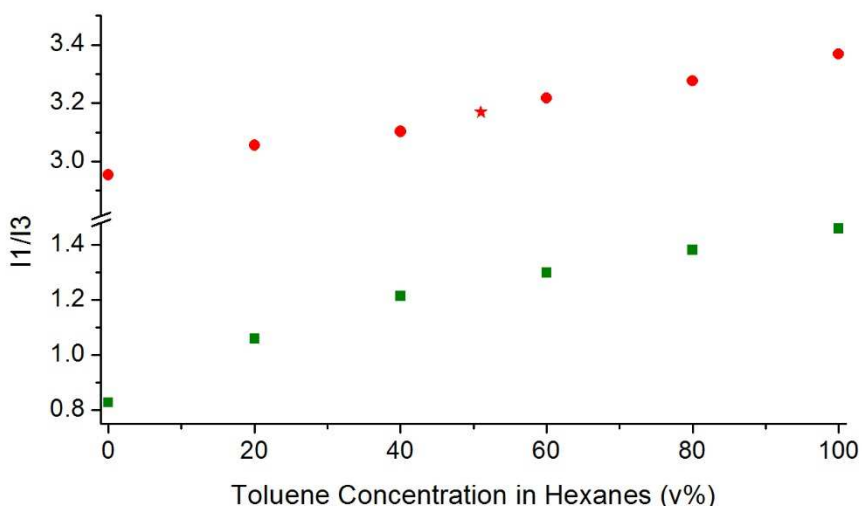
Figure S12. Polarity parameters (I_1/I_3) for 0.01 mg/mL 1-pyrenemethanol (■) and 1-pyrenebutanol (●) in binary solutions of toluene in hexane mixtures, compared to the polarity parameter of butylpyrene-tethered NPs (★, polarity parameter of 3.17) in water. NPs were composed of 1.8k PS core and 3.6k-b-16.6k PS-PEG as the stabilizing block copolymer. The NP measurements indicate the more hydrophobic butylpyrene terminal group (logP of 5.7) only samples only the core.

SI-VIII. Investigating the Effects of Quenching

Nile Red. To assure that the observed fluorescence emission spectra were not due to quenching or other energy transfer mechanisms, the average Nile Red mass fraction in our NPs was determined and compared against the critical mass fraction for the dye for the onset of quenching. The Förster radius of NR – the distance at which Förster resonance energy transfer becomes 50% efficient[8] – needs to be determined in order to calculate the critical mass fraction of NR, and is done using the following equation[8]:

$$R_0^6 = \frac{(9\ln 10)\kappa^2 Q_D}{128\pi^5 N_A n^4} \int_0^\infty F_D(\lambda)\varepsilon(\lambda)\lambda^4 d\lambda$$

where κ^2 is the orientation factor (2/3 for randomly oriented molecules), Q_D is the quantum yield for the dye (70%[9]), N_A is Avogadro's number, n is the refractive index of the material (here PS or PEG), F_D is the fluorescence spectrum of the dye (area normalized to 1), ε is the molar extinction coefficient of the dye, and λ is the wavelength in nm. Using this equation, the absorption data for NR, and numerically integrating using MATLAB, we are able to find the Förster radius, R_0, to be 3.47 nm for PS and 3.61 nm for PEG. Assuming that this is the critical distance unto which quenching will start to become a major factor, the volume per dye in our particles needs to be 41.8 nm^3 (PS). Based on the density of polystyrene (1.050 g/cm^3), there must be 4.39 x 10^{-20} g PS per Nile Red molecule (290 g/mol or 4.82 x 10^{-22} g/molecule), a critical NR mass fraction of 1.09 x 10^{-2} is found. Similarly, if the dye resides in the PEG corona (1.128 g/cm^3), then the critical NR mass fraction is 9.00 x 10^{-3}.

To determine the mass fraction of NR in our NPs, we divide our total mass of NR added by the total mass of PS or PEG in the system based on the formulations outlined in SI-II. Table S6 shows the maximum mass fraction of NR in the PS cores and PEG coronae of our particles based on PEG block M_W. For all PEG block MWs above 5.5k, NR mass fractions for the PS core and PEG corona are smaller than the critical NR mass fraction. However, for 5.5k PEG block MW, NR is distributed between the PS core and PEG corona in a 57:43 ratio (see Table S4). This would reduce the NR mass fraction below that of the critical mass fraction. Thus, we do not expect FRET to affect our NR fluorescence results.

Table S6. Maximum Mass Fraction of NR in the PS Cores and PEG Coronae of NR-tethered PS-PEG NPs

PEG Block M_W	Maximum NR Mass Fraction (x 10^3)	
	PS Core	PEG Corona
5.5k	9.83	16.1
16.6k	5.79	5.48
25k	4.41	3.66
36k	3.36	2.55
67k	2.01	1.38
Critical	10.9	9.00

Pyrene. Pyrene is known to form an excimer at around 20.8 cm^{-1} (480 nm), which will also decrease the fluorescence of Py monomers[10]. Hence, to assure that we are not affecting the results of our Py derivative-tethered NPs by excimer formation, we evaluate whether we have a significant contribution to the fluorescence of our NPs from a peak at around 480 nm. As can be seen in Figures S7 and S8, the fluorescence intensity at 480 nm is negligible (< 3%) in comparison to the primary Py peaks at around 377 nm. Therefore, Py excimers do not play a significant role in our experimental results.

SI-VIII. Investigating the Effects of Impurities.

As seen in Figures S3 and S4, there are impurities observed by ^{1}H NMR around 4.2 and 4.7 ppm. We attribute these impurities to residue from the (red) rubber septa, purchased from ChemGlass, used during the final reaction conjugating hydroxy functionalized dyes to our block copolymer. This reaction step is conducted under toluene reflux for 48 hours, and, although a condenser is placed between the reaction flask and the septum, there is a possibility that residue from the septum may be extracted by toluene vapors and condensed into the reaction. We have seen this before with other reactions we have conducted in toluene, DMF, and hexanes, which usually turn these reactions from clear to a yellow-brown. However, since our reactions were with dyes, we did not notice the contamination as it occurred.

To test whether these impurities appeared from the septum, we soaked a red rubber septum overnight in hexanes. The yellowed hexanes were then concentrated and dissolved in CDCl$_3$, resulting in NMR peaks similar to those seen in S3 and S4 between 4.2 and 4.7 ppm. We dissolved the same residue in dichloromethane and conducted UV-Vis absorption measurements that demonstrated no absorbance, relative to a blank, of the dissolved residue above 400 nm. This indicates that, although there was an impurity present from the red rubber septum in our dye-tethered copolymer, this impurity should not affect our fluorescent results.

Additionally, free dye may have an effect on our fluorescent results. However, we have found by TLC that our dye-tethered PS-PEG products only show one fluorescent spot at 0 RF, relative to 0.49 RF for HOMe$_2$NR developed in 2:1 EtOAc/IPA. This shows that no free dye is seen in our PS-PEG-dye products, and that free dye is not a concern for our experimental systems.

SI-IX. Supplemental Information References

1.   Debets, M. F.; Berkel, S. S. V.; Dommerholt, J.; Dirks, A. T. J.; Rutjes, F. P. J. T.; Delft, F. L. V., Bioconjugation with Strained Alkenes and Alkynes. *Accounts of Chemical Research* **2011,** *44* (9), 805-815.
2.   Gmehling, J.; Menke, J.; Krafczyk, J.; Fischer, K.; Fontaine, J.-C.; Kehiaian, H. V., Azeotropic Data for Binary Mixtures. In *CRC Handbook of Chemistry and Physics*, 95th ed.; Haynes, W. M., Ed. CRC Press/Taylor and Francis: Boca Raton, FL, 2013.
3.   Briggs, M. S. J.; Bruce, I.; Miller, J. N.; Moody, C. J.; Simmonds, A. C.; Swann, E., Synthesis of functionalized fluorescent dyes and their coupling to amines and amino acids. *Journal of the Chemical Society, Perkins Transactions 1* **1997,** *1*, 1051-8.
4.   Han, J.; Zhu, Z.; Qian, H.; Wohl, A. R.; Beaman, C. J.; Hoye, T. R.; Macosko, C. W., A simple confined impingement jets mixer for flash nanoprecipitation. *Journal of Pharmaceutical Sciences* **2012,** *101* (10), 4018-4023.
5.   Jose, J.; Burgess, K., Benzophenoxazine-based fluorescent dyes for labeling biomolecules. *Tetrahedron* **2006,** *62*, 11021-11037.
6.   Street, K. W.; Acree, W. E., The Py Solvent Polarity Scale: Binary Solvent Mixtures Used in Reversed-Phase Liquid Chromatography. *Journal of Liquid Chromatography* **1986,** *9* (13), 2799-2808.
7.   Budijono, S. J.; Russ, B.; Saad, W.; Adamson, D. H.; Prud'homme, R. K., Block copolymer surface coverage on nanoparticles. *Colloids and Surfaces A: Physicochemical and Engineering Aspects* **2010,** *360*, 105-110.
8.   Lakowicz, J. R., *Principles of Fluorescence Spectroscopy*. 3rd ed.; Journal of Biomedical Optics: 2006.
9.   Sackett, D. L.; Wolff, J., Nile red as a polarity-sensitive fluorescent probe of hydrophobic protein surfaces. *Analytical Biochemistry* **1987,** *167* (2), 228-234.
10.   Förster, T., Excimers. *Angewandte Chemie International Edition in English* **1969,** *8* (5), 333-343.